P5D.3 EVALUATION OF ICE CRYSTAL RIMING WITH WIND PROFILER AND IN-SITU OBSERVATIONS FROM THE ISPA EXPERIMENT

Stephen A. Cohn*[1], Douglas H. Lowenthal[2], Randolph D. Borys[2],
William O. J. Brown[1], and James O. Pinto[1]

[1]National Center for Atmospheric Research, Boulder, CO, USA
[2]Desert Research Institute, Reno, NV, USA

1. INTRODUCTION

As ice crystals fall through super cooled liquid water (SLW) and cloud droplets freeze (rime) onto the crystals, their mass will increase. Further, as the crystals' mass increases their terminal fall velocity will increase (Locatelli and Hobbs 1974). Crystal fall speed is also a function of the crystal size (usually expressed in terms of diameter) and crystal habit. But in general, it is reasonable to expect that ice crystals with a greater amount of riming will be observed to have a larger terminal velocity.

The 2001 and 2002 Inhibition of Snowfall by Pollution Aerosols (ISPA) experiments provide an opportunity to re-examine the relationship between ice crystal degree-of-riming and terminal fall speed. A detailed empirical examination of this relationship has been reported by Mosimann (1995), with additional conclusions presented in Mosimann and Steiner (1992) and Mosimann et al. (1993, 1994). However, their results are limited to observations on Mount Rigi in Switzerland. This paper makes use of similar methodology but the ISPA data set was collected on Mt. Werner in Steamboat Springs, Colorado. The preliminary analysis presented here qualitatively confirms earlier results that a correlation exists between riming and fall speed.

2. PRIOR RESULTS FROM MOUNT RIGI

Analysis and results presented by Mosimann (1995) make use of data from the "Winter Precipitation at Mount Rigi" (WPMR) project (Staehelin et al. 1993). At two in-situ stations on Mount Rigi ice crystal samples were collected during periods of snowfall. One site was near the top of the mountain while the second site was about half way down its side. Visual examination of crystal samples, as described in Mosimann et al. (1994), was used to classify the degree of riming of each according to the definitions in Table 1 (after Mosimann et al. 1994). Note that the degree-of-riming scale is actually continuous and the visual examination used the discrete entries of the table as reference points.

Degree of Riming	Description
0	Unrimed (no cloud droplets)
1	Lightly rimed, (<25% covered)
2	Moderately rimed (about 50%)
3	Densely rimed (about 100%)
4	Heavily rimed (multiple layers)
5	Graupel

Table 1: Definition of each degree of riming, summarized from Mosimann et al. (1994).

Simultaneous measurements were made of ice crystal fall speed (relative to the ground) with a vertically pointing X-band radar. This radar was located about 3.5 km west of the upper in situ station.

A scatter plot of degree of riming vs. crystal fall speed showed a weak but clear relationship, which the WPMR investigators approximate with (1)

$$R = \sqrt{10.9v - 8.1} \qquad (1)$$

In (1) R is the degree of riming and v is the ensemble average fall speed in m s^{-1}. In the WPMR implementation, v was averaged over 5-minute intervals.

3. RESULTS FROM ISPA

The ISPA experiment was designed to investigate a relationship between snowfall

---

* Corresponding author address: Stephen A. Cohn, National Center for Atmospheric Research, P.O. Box 3000, Boulder, CO 80307-3000; e-mail: cohn@ucar.edu.

rate and aerosol induced changes in the cloud droplet size distribution (Borys et al. 2003). The experimental configuration was similar in many ways to the WPMR project. In situ measurements were collected at the Storm Peak Laboratory (SPL, Borys and Wetzel 1997) which is located at the 3210 m MSL summit of Mt. Werner near Steamboat Springs, Colorado. At the same time the MAPR radar wind profiler (Cohn et al. 2001) measured ice crystal fall speed in the valley 6.5 km to the west. MAPR was located at 2067 m MSL, or about 1150 m lower than SPL. Although ice crystal images were recorded at SPL to allow for visual determination of crystal habit and riming, for the present analysis the degree of riming is found from the relative concentration of SO_4 in the ice crystal and in cloud droplets collected at the same time. This method of determining a rimed mass fraction (RMF) is suitable in situations where the seeder-feeder mechanism takes place (e.g. Choularton and Perry 1986). It relies on the rimed mass coming from an orographically generated (feeder) polluted cloud and the non-rimed mass originating from a clean cloud aloft (seeder). This method has been shown to be valid at SPL (Borys et al. 2000). During the two ISPA field seasons there were 78 in situ data collection periods with approximate durations of 20-40 minutes. During these periods SPL was typically within the feeder cloud with precipitation falling.

Equation 1 was generated for the altitude of Mount Rigi. For fall speed measurements at other altitudes, it is necessary to introduce a correction, because ice crystal terminal velocity is a function of air density (approximately $\rho^{0.4}$), Equation 2 is found by translating (1) to a reference pressure of 1000 hPa

$$R = \sqrt{11.9v - 8.1} \qquad (2)$$

In the remainder of this paper, v measured at SPL is corrected to this reference altitude before relating the fall speed to a degree of riming.

Before proceeding it is useful to address a concern which was noted by Mosimann (1995). While the expected degree of riming is correlated with the terminal velocity of the ice crystal relative to the air, the radar measures this velocity relative to the ground. If there is vertical air motion, it will bias the result. To address this in the WPMR project, Mosimann introduced a “convective index” (based on temporal variation in observed fall speeds) which was used to identify times when there was an indication of significant vertical air motion. These times were not used when generating (1). This convective index was found to be inadequate for the ISPA data set because persistent vertical air motions are present due to orographic lifting in addition to any embedded convective cells. Therefore, for preliminary analysis of the ISPA data, a subjective evaluation is made based on visual inspection of the time-height plot of measured fall speeds. Observation periods with evidence of vertical air motions are not used, and this results in the loss of a large number of data collection periods. An alternative solution is proposed in section 4.

Using (2), the ISPA data is examined for a correspondence between R and the RMF determined from SO_4 concentrations. This result is shown in Fig. 1. In this figure each point corresponds to R and RMF measurements during one of 33 data collection periods. The remaining 45 periods were removed either because of visual evidence of vertical air motions (biasing R) or evidence of sample contamination (invaliding the RMF calculation). In this figure, R was computed using one-minute integrations of measured ice crystal fall speed, these one-minute values were smoothed to 5-minutes, and the maximum value of the smoothed R during the (typically 20-40 minute) observation period was chosen as representative of the period. The maximum was chosen, rather than the mean or median, because periods of heavy snow contribute most to the integrated value of RMF while periods of light snow contribute least. Therefore, the largest values are emphasized.

Note that R and RMF are not expected to be strictly linearly related. As riming increases, an ice crystal would asymptotically approach an RMF value of 1 when the rimed mass greatly exceeds the initial crystal mass. But even a crystal with a much lower RMF, for example equal rimed and unrimed mass (RMF=0.5), would probably be visually classified as graupel (R=5).

Fig. 1 shows that a fair degree of correlation exists between R and RMF. This is encouraging because the removal of points with evidence of vertical air motion was done by visual inspection and is therefore not an objective process. It is also worth noting that the removal of points with suspected vertical motions probably biases the remaining data toward light wind cases.

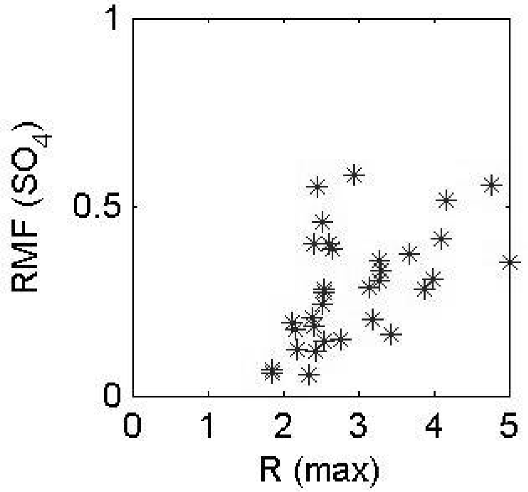

Figure 1: Degree of riming (R) determined from MAPR fall speed vs. rimed mass fraction (RMF) determined from in-situ measurements.

An issue which was not addressed by Mosimann is the possibility of a bias caused by the spatial separation of the radar measurement and the *in situ* measurement. In the case of the ISPA experiments, it is expected that riming occurs as “seeder” ice crystals from above fall through a “feeder” cloud containing SLW. This feeder cloud (which is expected to contain higher concentrations of SO$_4$) is generated by orographic lifting as the generally easterly flow nears Mt. Werner. It is expected that the riming rate, which depends on the SLW cloud drop distribution, will be similar throughout the feeder cloud. However, the residence time in the cloud may be different at SPL than at 1.1 km over MAPR. This difference is not investigated or accounted for in our analysis.

4. CORRECTION FOR AIR MOTION

During the 2002 ISPA data collection, a co-located wind profiler with a slightly higher frequency than MAPR (1299 MHz as opposed to 915 MHz) was also measuring fall speeds and full Doppler spectra. While there is some prospect that spectral differences between these two radars can be used to separately measure the vertical air motion and ice crystal terminal velocity, so far these efforts have not been successful. However, also during the 2002 ISPA data collection, the MM5 numerical model was run with a high resolution domain over the experimental site. From model forecasts, values of U (eastward velocity) and W (vertical air velocity) were found for each of 43 available observation periods. In the preliminary analysis these values were found graphically, but will be found numerically in future work. The eastward velocity was chosen because this direction is approximately perpendicular to the broad slope of Mt. Werner. Fig. 2 shows that the model predicts a relationship between U and W. Although there is some scatter, this result can be approximated as

$$\begin{aligned} W &= 0.1U - 0.5 \quad &; U \geq 5 \\ W &= 0 \quad &; U < 5 \end{aligned} \qquad (3)$$

where U and W are in m s^{-1}. This relation is also plotted as the line in Fig. 2.

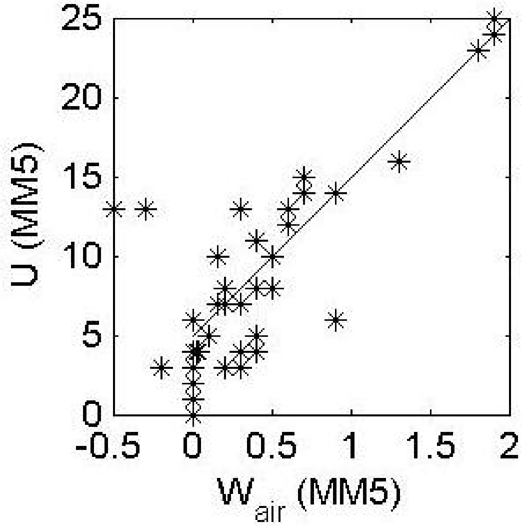

Figure 2: Vertical air motion (W$_{air}$) and eastward component of wind (U) predicted by the MM5 model during 43 ISPA observation periods. Units are m s^{-1}.

Because MAPR is a spaced antenna wind profiler, it uses a continuously vertically pointing beam to measure vertical motions. It simultaneously measures the horizontal wind using a full correlation analysis technique. Using (3) to represent the vertical air velocity induced as a function of measured eastward wind speed, the MAPR measurements of horizontal wind can be used to estimate the vertical air motion during the ISPA observation periods.

Fig. 3 is similar to Fig. 1 but the degree of riming is calculated after corrected for this estimated vertical air motion. This figure contains more points than Fig. 1 because observation periods are no longer removed based on evidence of vertical air motions. However, other observation periods are not included due to unavailability of a horizontal wind measurement.

Fig. 3 shows a comparable degree of skill as Fig 1. It is possible that introducing the additional computation based on horizontal wind speed adds an additional source of variance to the calculations. However, these calculations are preliminary, and firm conclusions are avoided pending a more rigorous analysis.

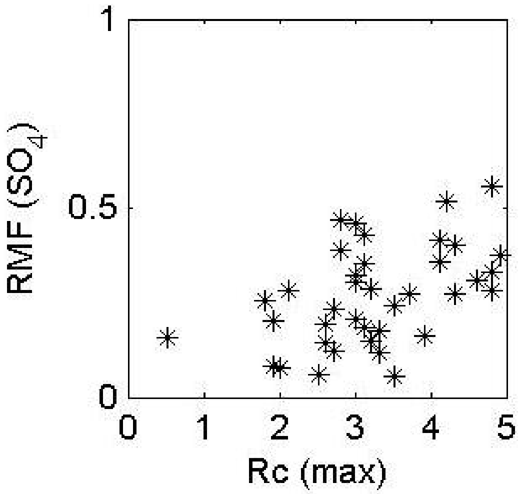

Figure 3: Degree of riming (Rc) determined from MAPR fall speed corrected for vertical air motion vs. rimed mass fraction (RMF) determined from in-situ measurements.

ACKNOWLEDGEMENTS

This work was supported by the NSF Division of Atmospheric Sciences grant ATM-0004265. Logistical assistance from the Steamboat Ski and Resort Corporation is greatly appreciated. NCAR is operated by the University Corporation for Atmospheric Research under sponsorship of the National Science Foundation.

REFERENCES

Borys, R. D., D. H. Lowenthal, S. A. Cohn, and W. O. J. Brown, 2003: Mountaintop and radar measurements of anthropogenic aerosol effects on snow growth and snowfall rate, *Geophys. Res. Lett.*, **30**, .

Borys, R. D., D. H. Lowenthal, and D. L. Mitchell, 2000: The relationships among cloud microphysics, chemistry, and precipitation rate in cold mountain clouds, *Atmos. Environment*, **34**, 2593-2602.

Borys, R. D., and M. A. Wetzel, 1997: Storm Peak Laboratory: A research, teaching and service facility for the atmospheric sciences, *Bull. Amer. Meteorol. Soc.*, **78**, 2115-2123.

Choularton, T. W., and S. J. Perry, 1986: A model of the orographic enhancement of snowfall by the seeder-feeder mechanism, *Quart. J. Roy. Meteor. Soc.*, **112**, 335-345.

Cohn, S. A., W. O. J. Brown, C. L. Martin, M. S. Susedik, G. Maclean, and D. B. Parsons, 2001: Clear air boundary layer spaced antenna wind measurements with the Multiple Antenna Profiler (MAPR), *Annales Geophysicae*, **19**, 845-854.

Locatelli, J. D., and P. V. Hobbs, 1974: Fall speed and masses of solid precipitation particles, *J. Geophys. Res.*, **79**, 2185-2197.

Mosimann, L., 1995: An improved method for determining the degree of snow crystal riming by vertical Doppler radar, *Atmos. Res.*, **37**, 305-323.

Mosimann, L., and M. Steiner, 1992: Prediction of cloudwater to precipitation ion concentration ratio by vertical Doppler radar, *Proc. 11th Conf. Clouds and Precipitation*, Montreal, Canada, pp. 892-894.

Mosimann, L., M. Steiner, and W. Henrich, 1993: Prediction of snow crystal shape and riming by vertical Doppler radar, *Atmos. Res.*, **29**, 85-98.

Mosimann, L., E. Weingartner, and A. Waldvogel, 1994: An analysis of accreted drop sizes and mass on rimed snow crystals, *J. Atmos. Sci.*, **51**, 1548-1558.

Staehelin, J., A. Waldvogel, J. L. Collett Jr., R. W. Dixon, W. Heimgartner, W. Henrich, C. Hsu, L. Li, L. Mosimann, B. Oberholzer, A. S. H. Prevot, W. Schmid, T. Schumann, M. Steiner, M. Volken, and B. Zinder, 1993: Scientific goals and experiments of the project “Winter Precipitation at Mount Rigi”: An overview, *Water, Air, Soil Pollution*, **68**, 1-14.